Pyrazole appended quinoline-BODIPY based arene ruthenium complexes: their anticancer activity and potential applications in cellular imaging

Rajendra Prasad Paitandi[a], Vinay Sharma[b], Vishwa Deepak Singh[a], Bhupendra Kumar Dwivedi[a], Shaikh M. Mobin[b,c,d], and Daya Shankar Pandey*[a]

[a]Department of Chemistry, Institute of Science, Banaras Hindu University, Varanasi - 221005 (UP), India.

[b]Discipline of Biosciences and Bio-Medical Engineering, Indian Institute of Technology Indore, Simrol, Indore-453552, India.

[c]Discipline of Chemistry, Indian Institute of Technology Indore, Simrol, Indore-453552, India.

[d]Metallurgical Engineering and Material Science, Indian Institute of Technology Indore, Simrol, Indore-453552, India.

Contents

1. NMR spectra of the **L1**…….....S2
2. NMR spectra of the complexes**1**–**4**.....S3-S6
3. ESI-MS of the **L1** and complexes**1**–**4**…….....S7-S8
4. UV-Vis spectra of DNA in presence of **1**–**3**.....S9
5. Emission spectra from EB bound DNA with **1**, **2** and **3**.....S10
6. The plot of [DNA]/($\varepsilon_a-\varepsilon_f$) vs. [DNA] for **1**–**4** from UV-Vis study.....S11
7. Stern-Volmer plot for fluorescence titrations of EB-DNA with **1**–**4**.....S11
8. Fluorescence lifetime spectra of ligands **L1**–**L2** and complexes **1**–**4**.....S11
9. Cyclic voltammogram of ligands **L1–L2** and complexes **1**–**4**.....S12-S13
10. Hydrolysis study of complex **2**.....S13
11. UV-Vis titrations spectra of complexes **2** and **4** in dark and light in PBS…….. …….S14
12. DFT optimized structures and Frontier MOs contour plo**1**–**3**.....S15
13. Molecular docking of **1**–**3** with DNA …….....S16-S17
14. The spectral changes in DPBF treated with **1**–**3**…….....S17
15. Flow cytometer analysis of DCFDA treated with **1**–**3** on HeLa cells.....S18
16. Fluorescence microscopic images of HeLa cells using LysoTracker Red in the presence of complexes **1–3**.....S19
17. Fluorescence microscopic images of HeLa cells using MitoTracker Red in the presence of complexes **1–3** S20
18. Tables S1-S5.....S21-S23

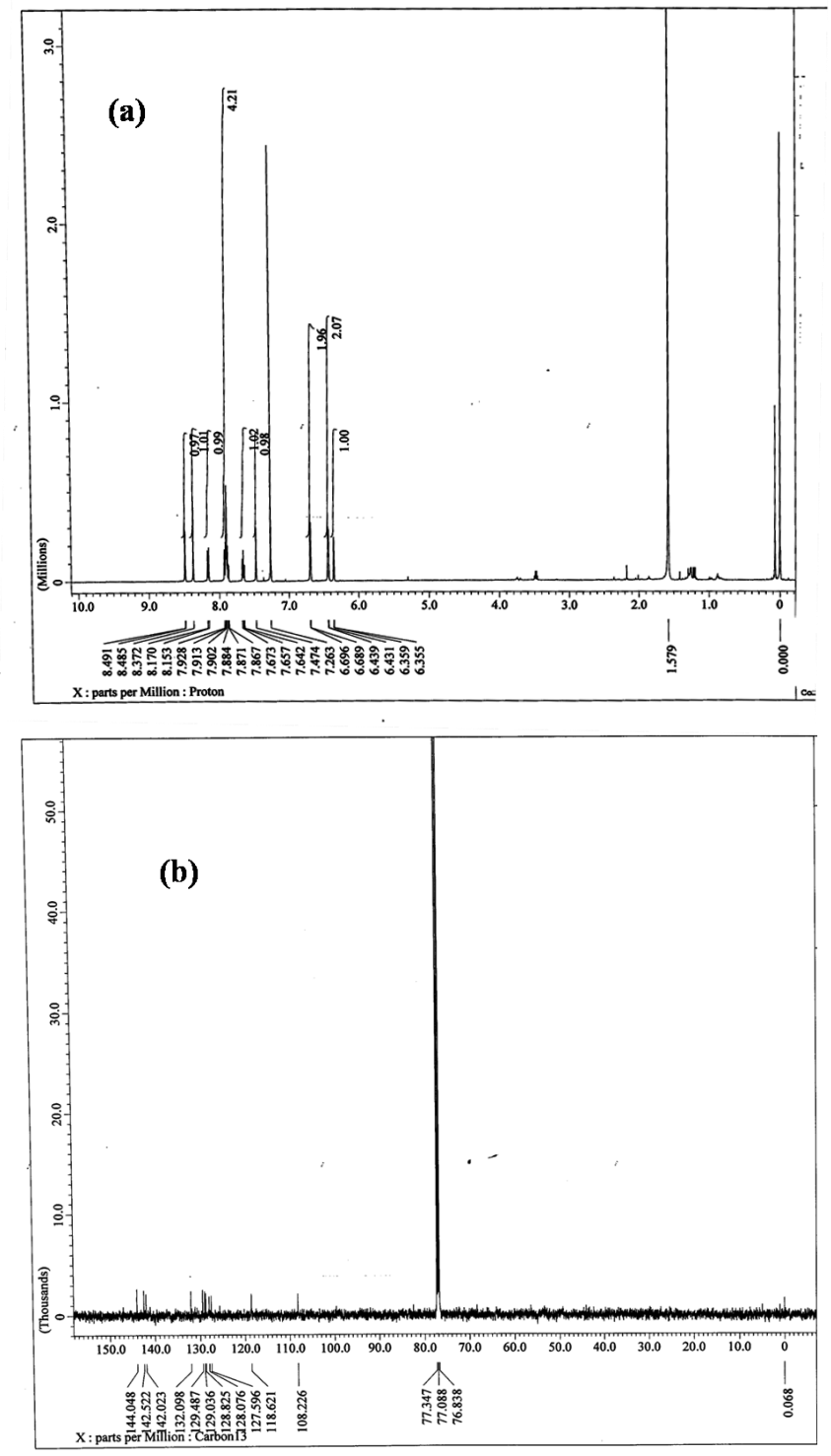

Fig. S1 ^{1}H (a) and ^{13}C (b) NMR spectra of **L1** in $CDCl_3$.

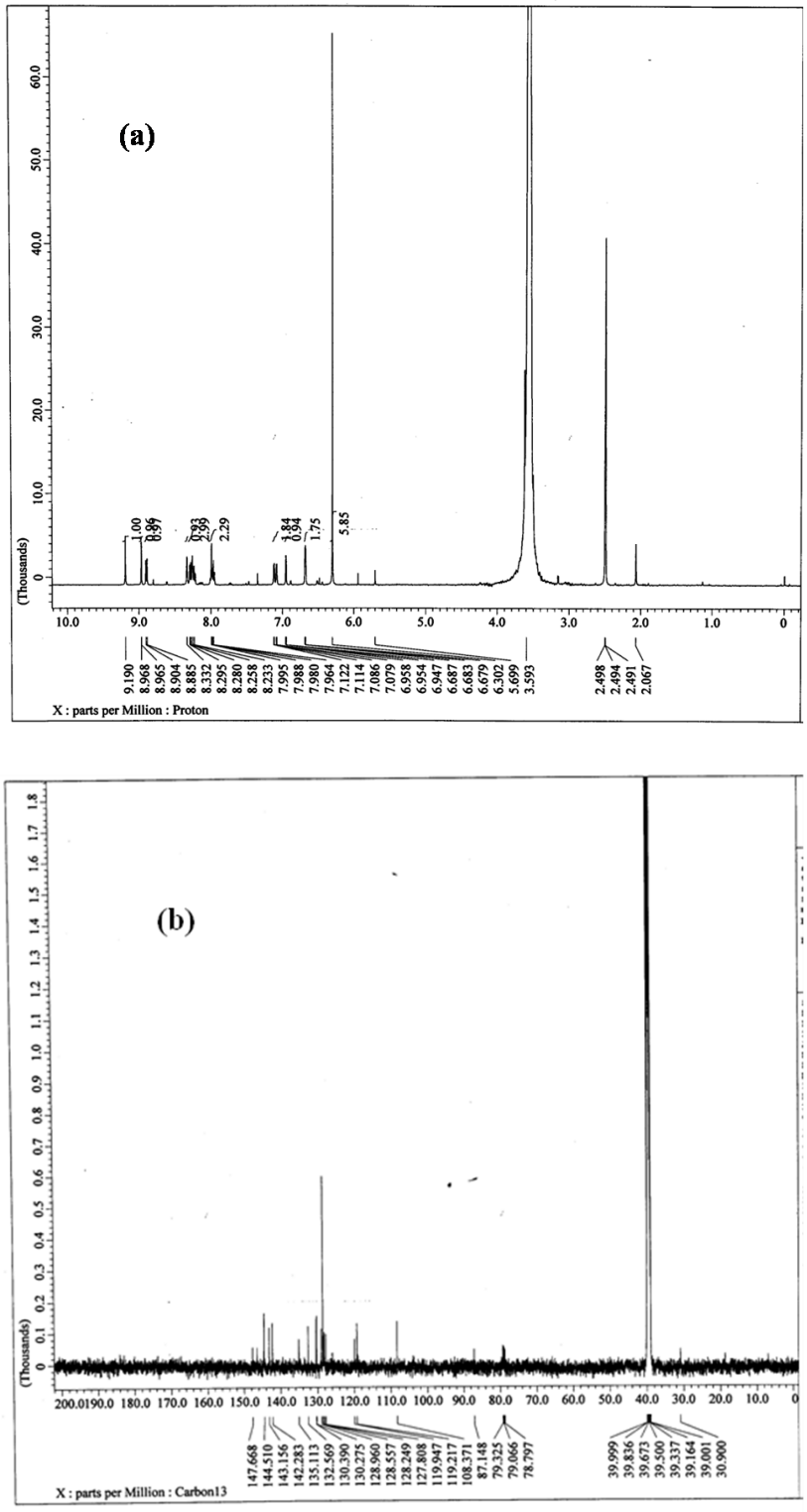

Fig. S2 ^{1}H (a) and ^{13}C (b) NMR spectra of **1** in DMSO-d_6.

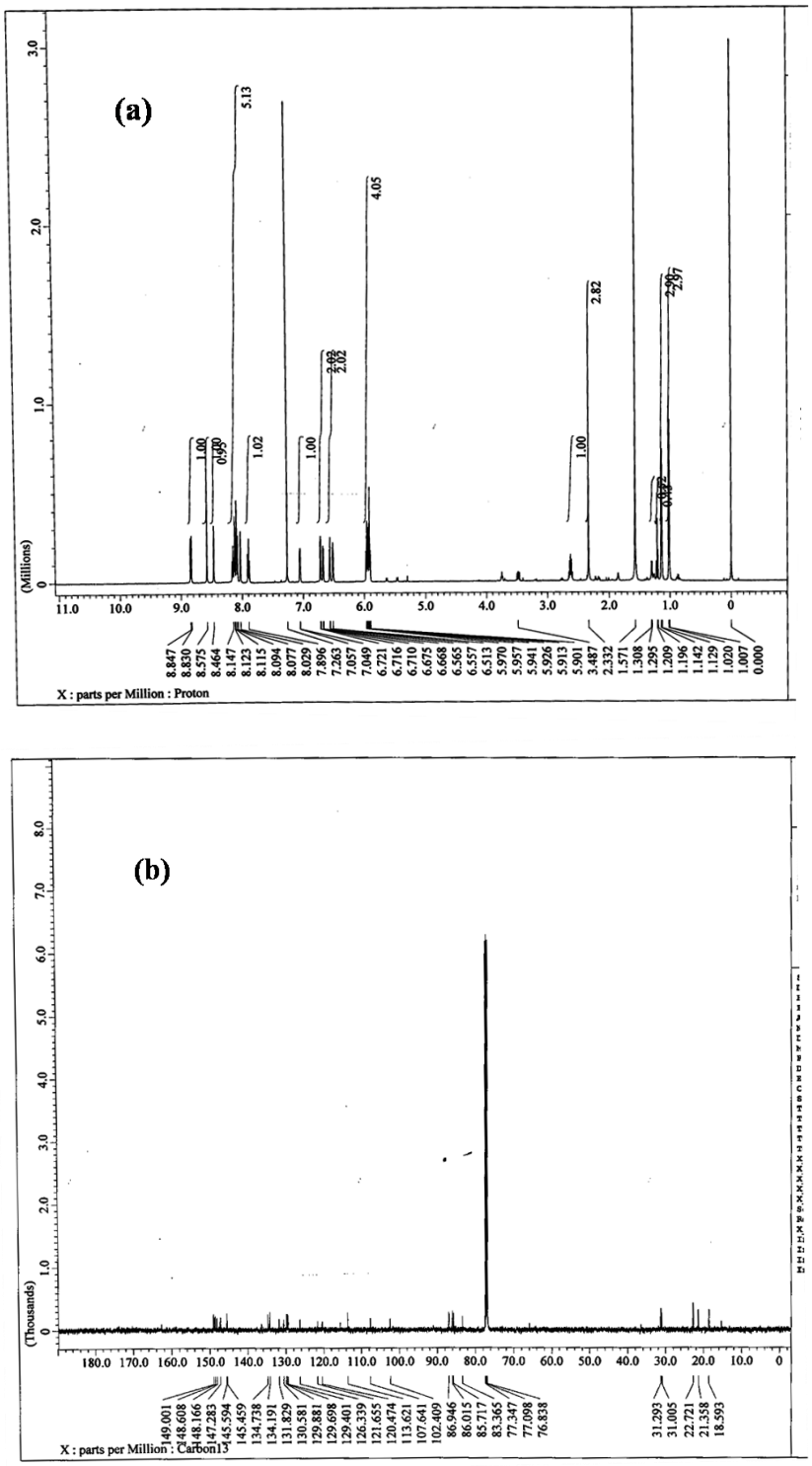

Fig. S3 ^{1}H (a) and ^{13}C (b) NMR spectra of **2** in $CDCl_3$.

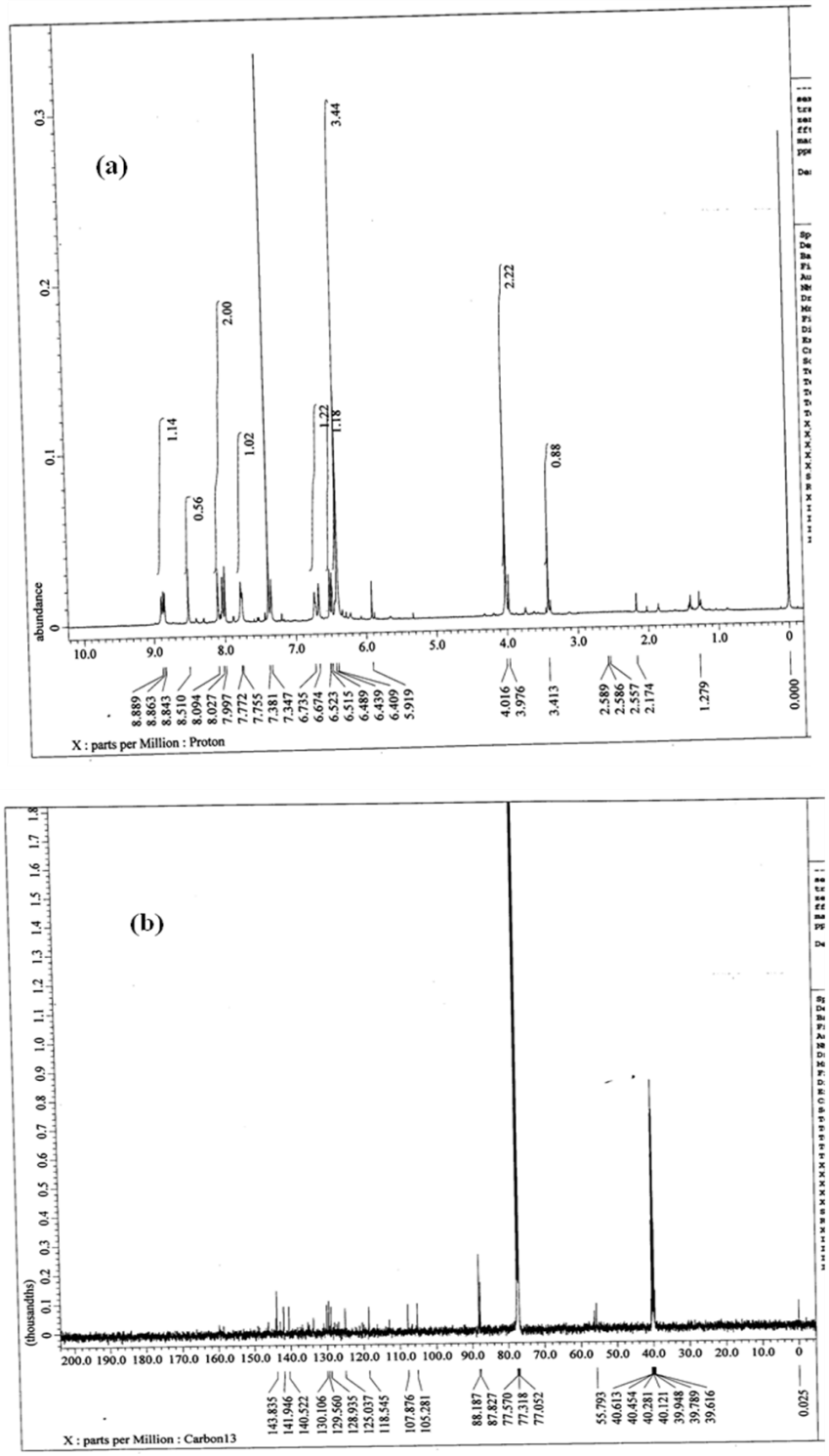

Fig. S4 ^{1}H (a) and ^{13}C (b) NMR spectra of **3** in $CDCl_3$.

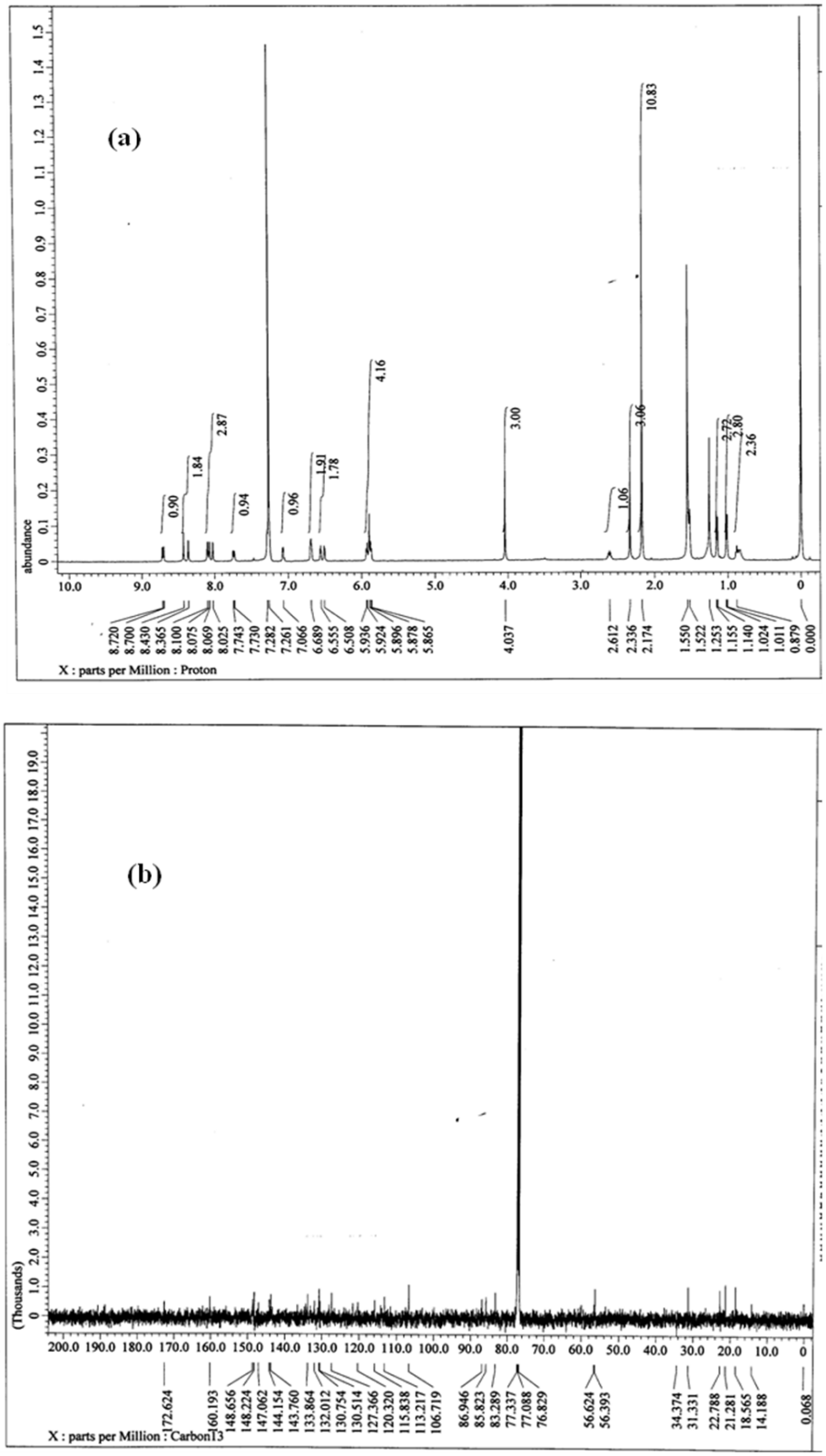

Fig. S5 ^{1}H (a) and ^{13}C (b) NMR spectra of **4** in $CDCl_3$.

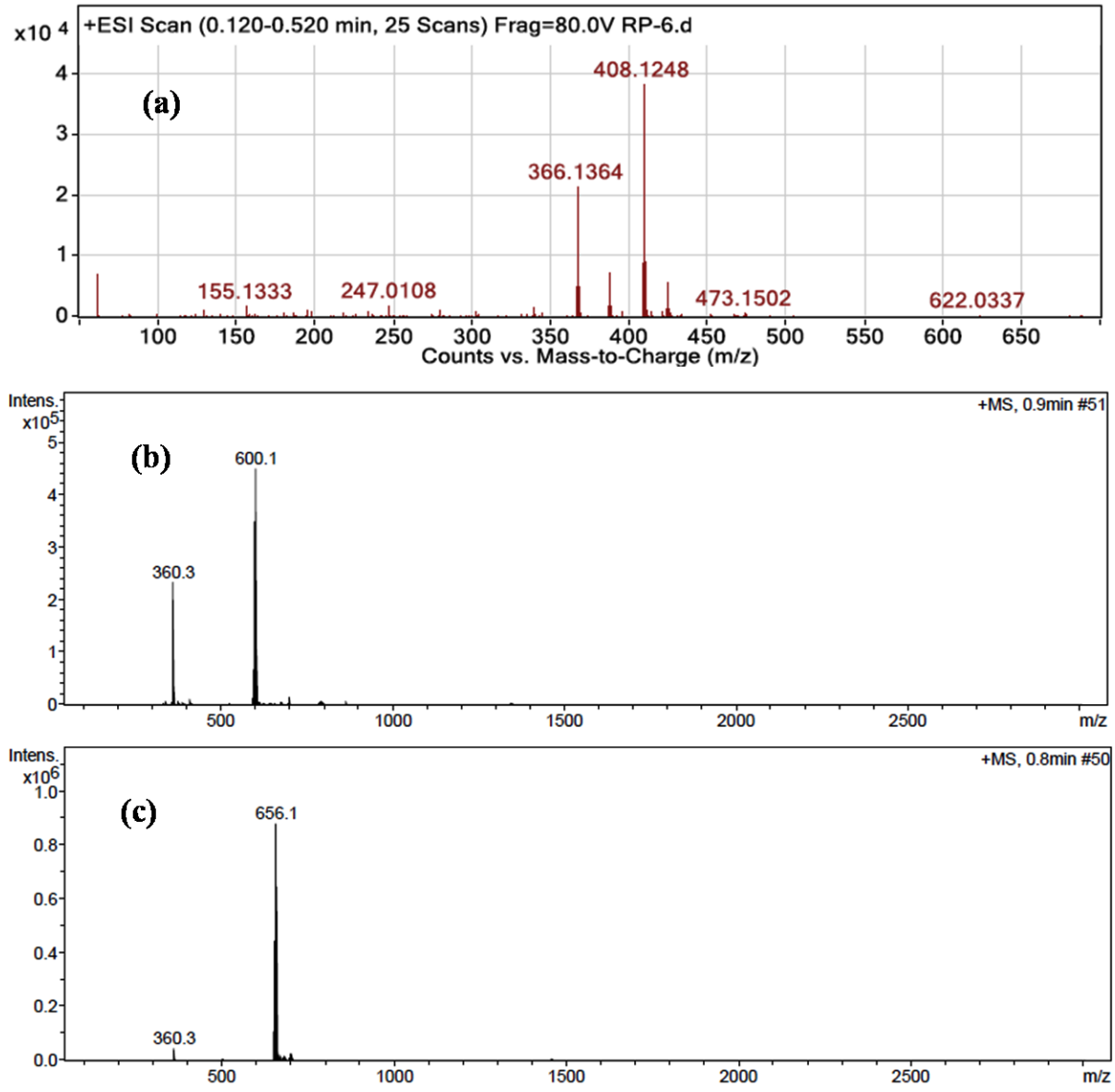

Fig. S6 ESI-MS spectra of **L1** (a), **1** (b) and **2** (c).

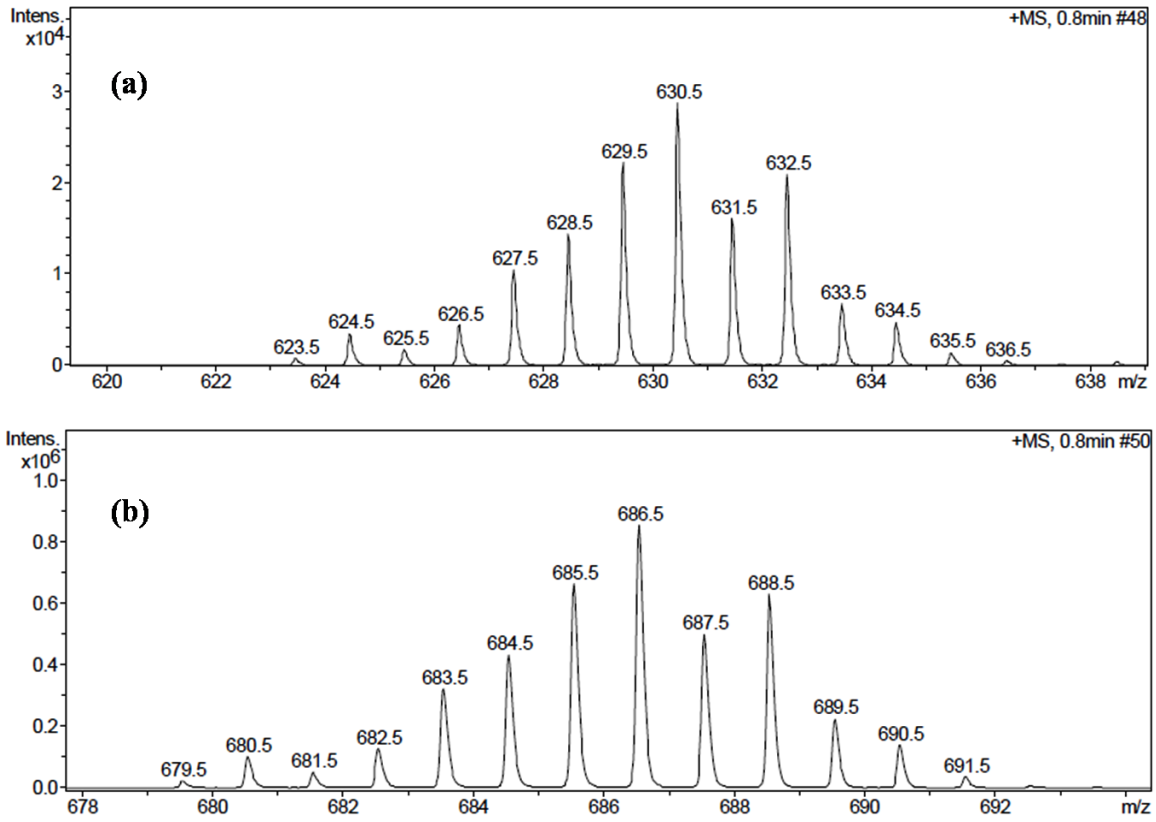

Fig. S7 ESI-MS spectra of **3** (a) and **4** (b).

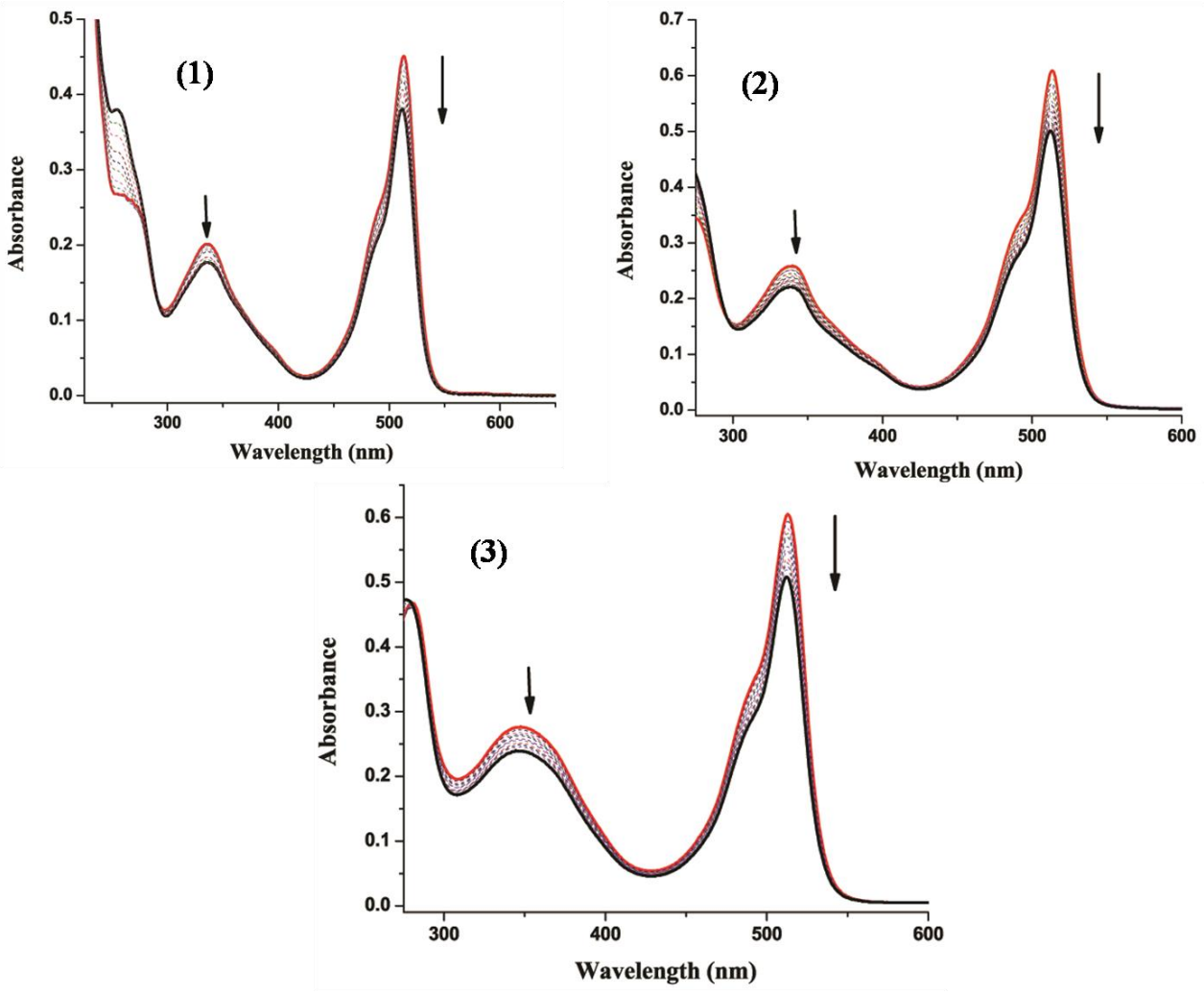

Fig. S8 UV–Vis spectra of **1–3** in PBS with increasing concentrations of CT-DNA (0–20 μM) at room temperature. Arrow shows absorbance changes with increasing CT-DNA concentration.

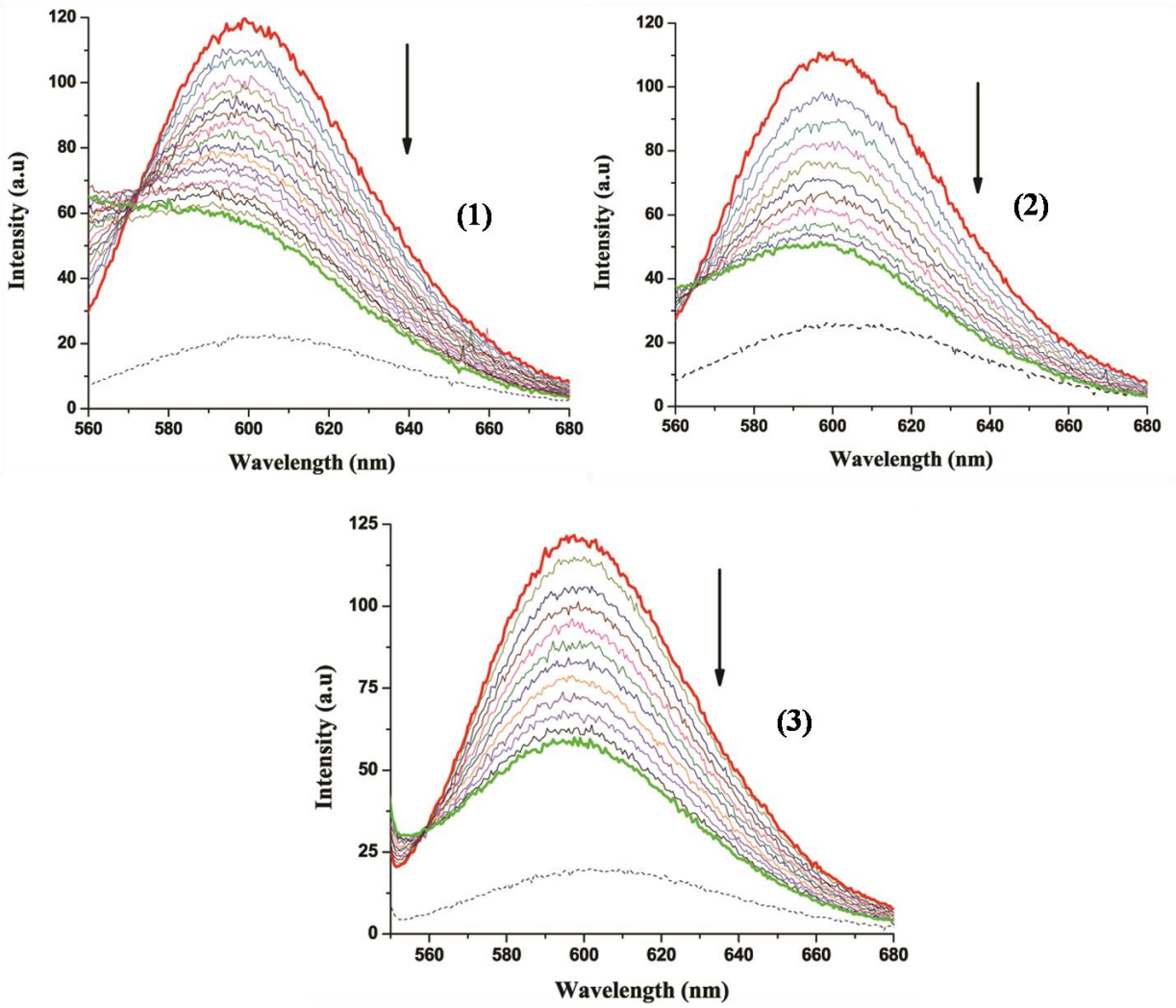

Fig. S9 Emission spectra of DNA–EB system in absence (--- black line) and presence of **1–3** [EB = 10 μM, [DNA] = 100 μM, [**1–3**] = 0–50 μM]. Arrow shows changes in emission intensity upon addition of increasing concentration of the complexes.

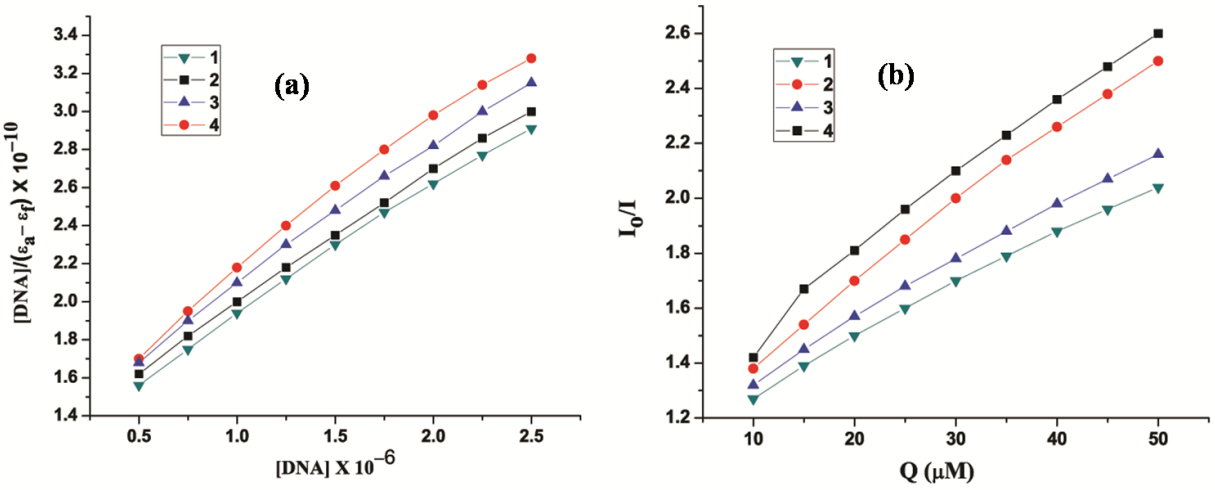

Fig. S10 (a) Plot of [DNA]/($\varepsilon_a - \varepsilon_f$) vs. [DNA] for **1**–**4** from UV-Vis (b) Stern-Volmer plots of the EB-DNA fluorescence titration for complexes **1**–**4.**

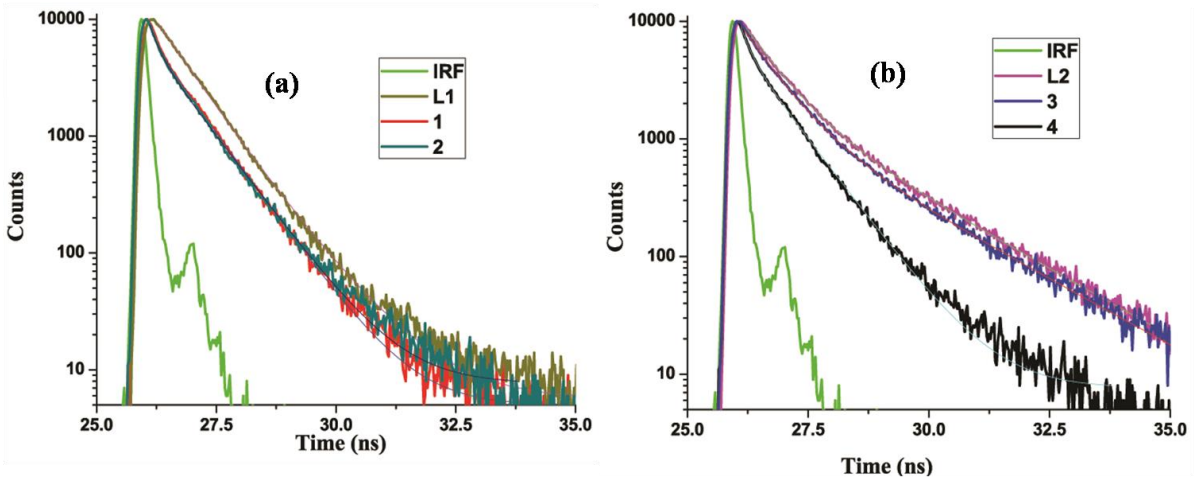

Fig. S11 Fluorescence lifetime spectra of **1**–**2** and **L1 (a)** and **3**–**4** and **L2 (b)** in pure acetonitrile.

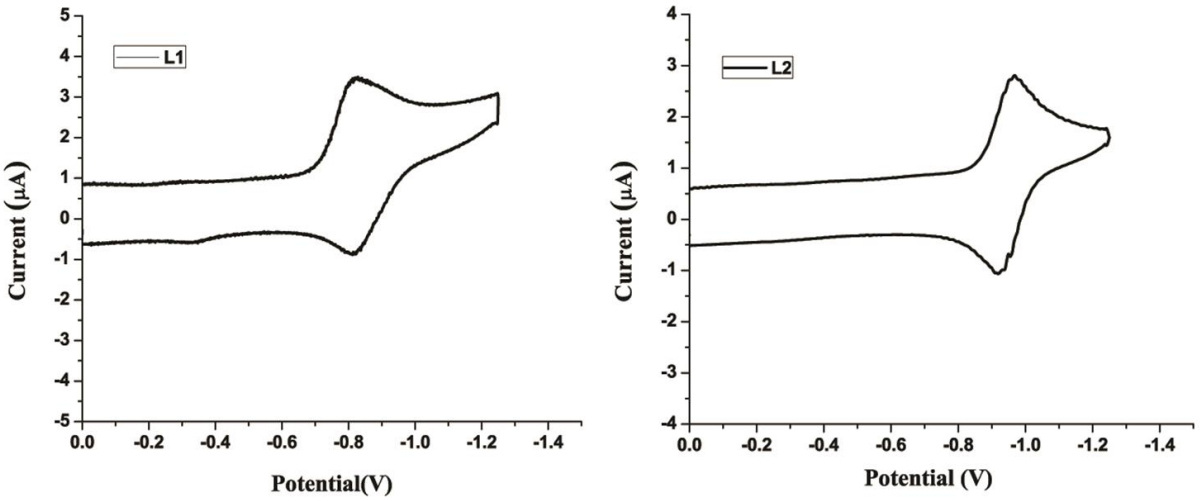

Fig. S12 Cyclic voltammogram of **L1** (a) and **L2** (b) in CH_3CN (*c*, 100 μM) at room temperature.

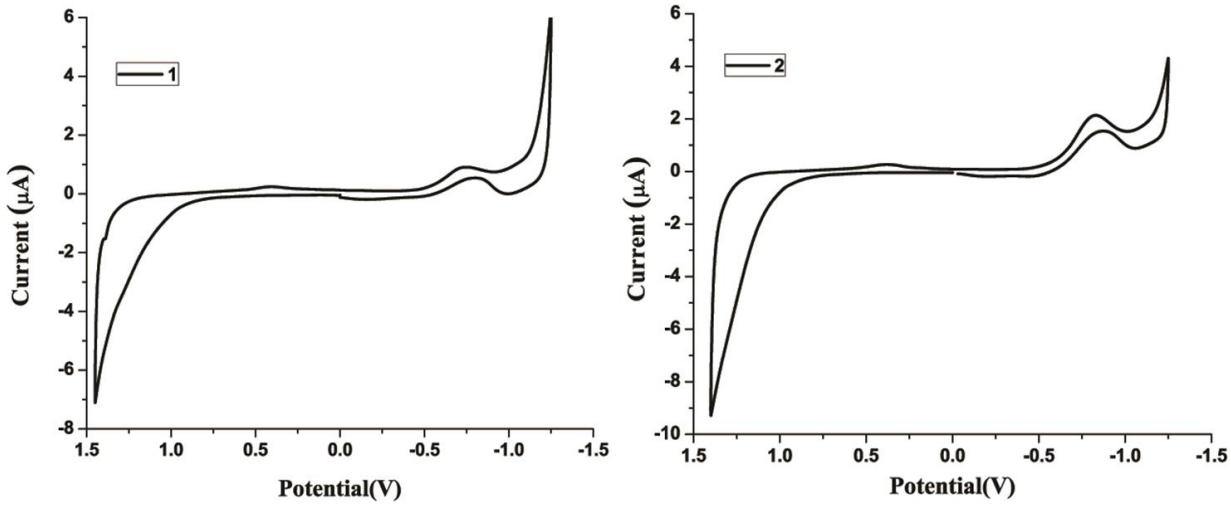

Fig. S13 Cyclic voltammogram of **1** (a) and **2** (b) in CH_3CN (*c*, 100 μM) at room temperature.

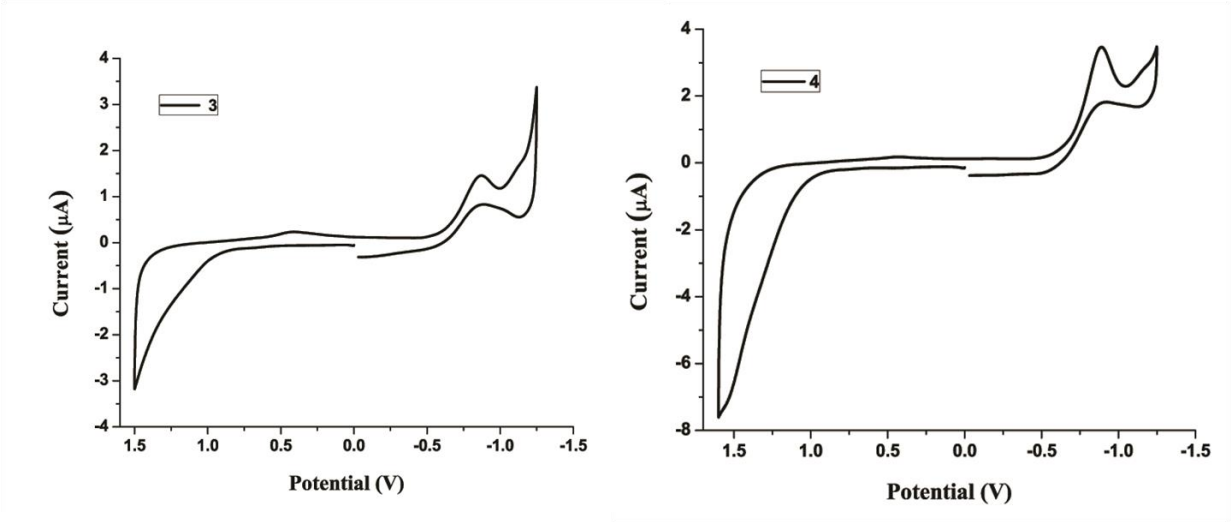

Fig. S14 Cyclic voltammogram of **3** (a) and **4** (b) in CH_3CN (*c*, 100 μM) at room temperature.

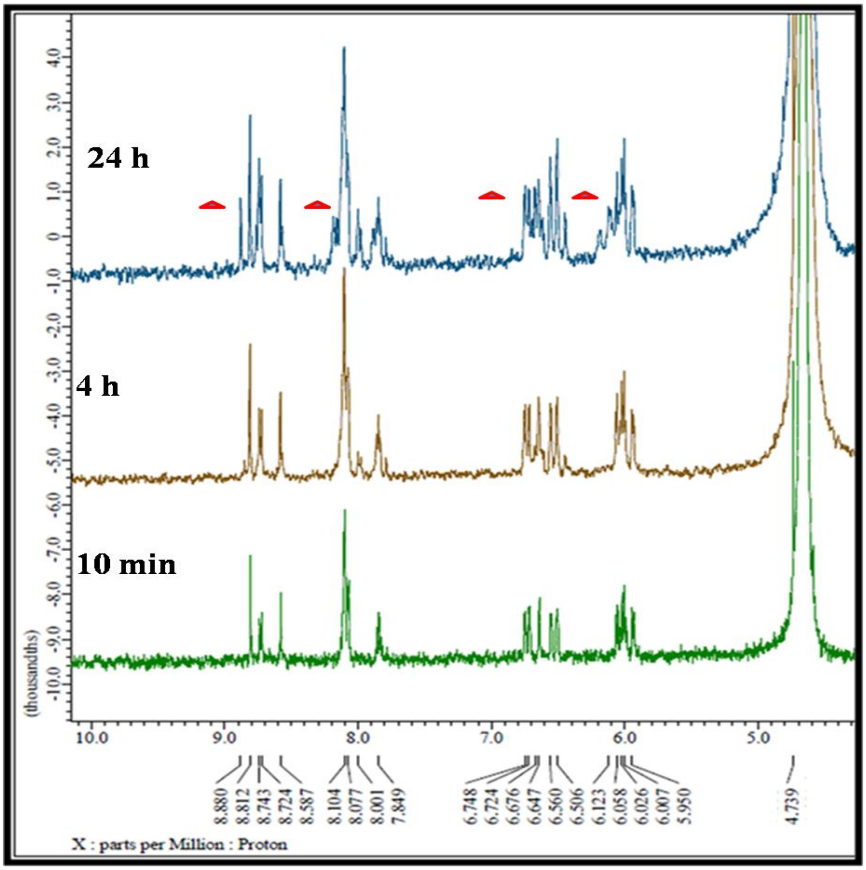

Fig. S15 Hydrolysis of **2** in 5% DMSO-d_6/95% D_2O (v/v) at 293K over a period of 24 h monitored by ^1H NMR; peaks labelled as (▲) correspond to the aqua complex after hydrolysis.

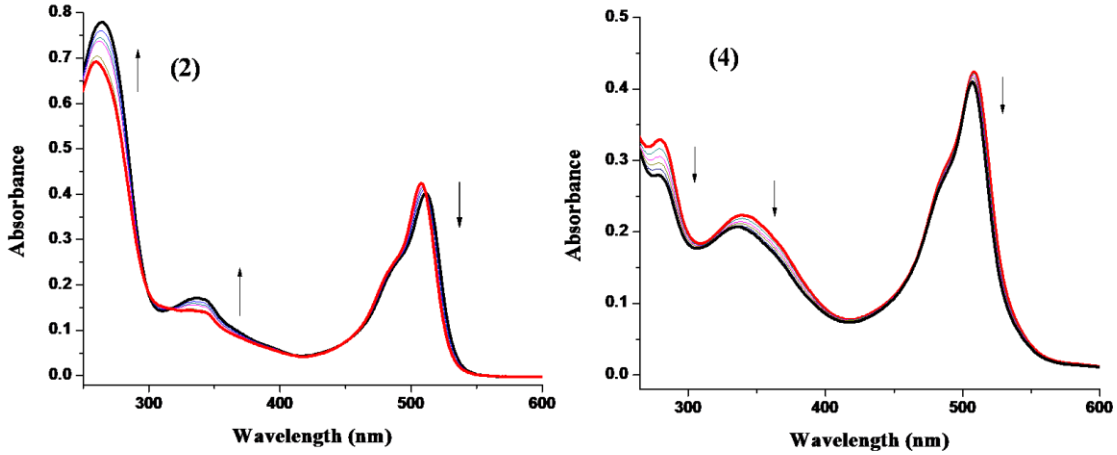

Fig. S16 UV-Vis spectrum for a 10 μM solution of complexes **2** and **4** (dark) in PBS (1% DMSO) recorded over 12 h at 298 K.

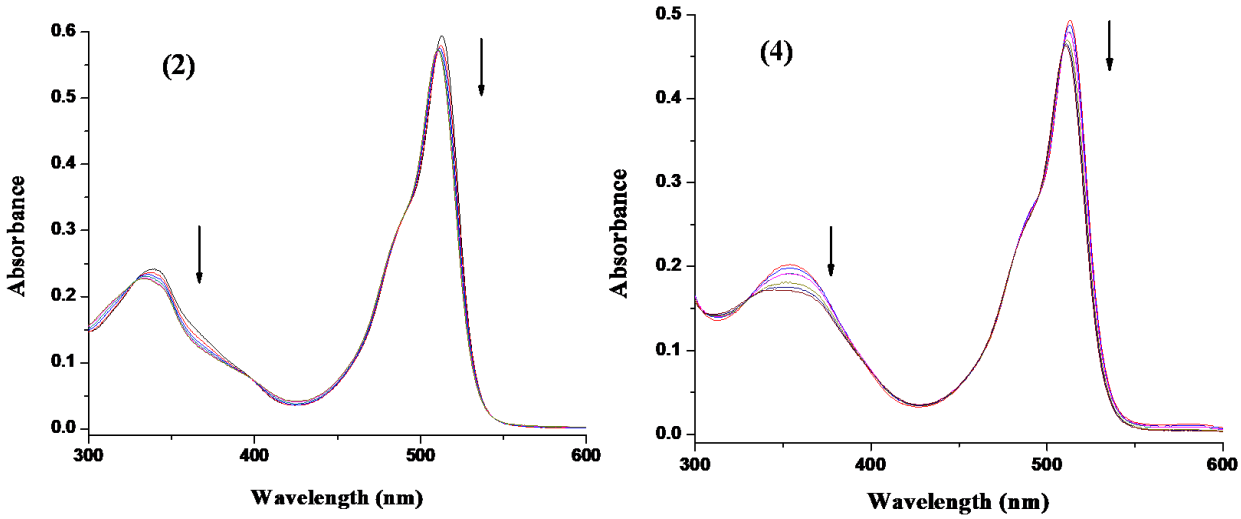

Fig. S17 UV-Vis spectrum for a 10 μM solution of complexes **2** and **4** (light) in PBS (1% DMSO) recorded over 2 h at 298 K.

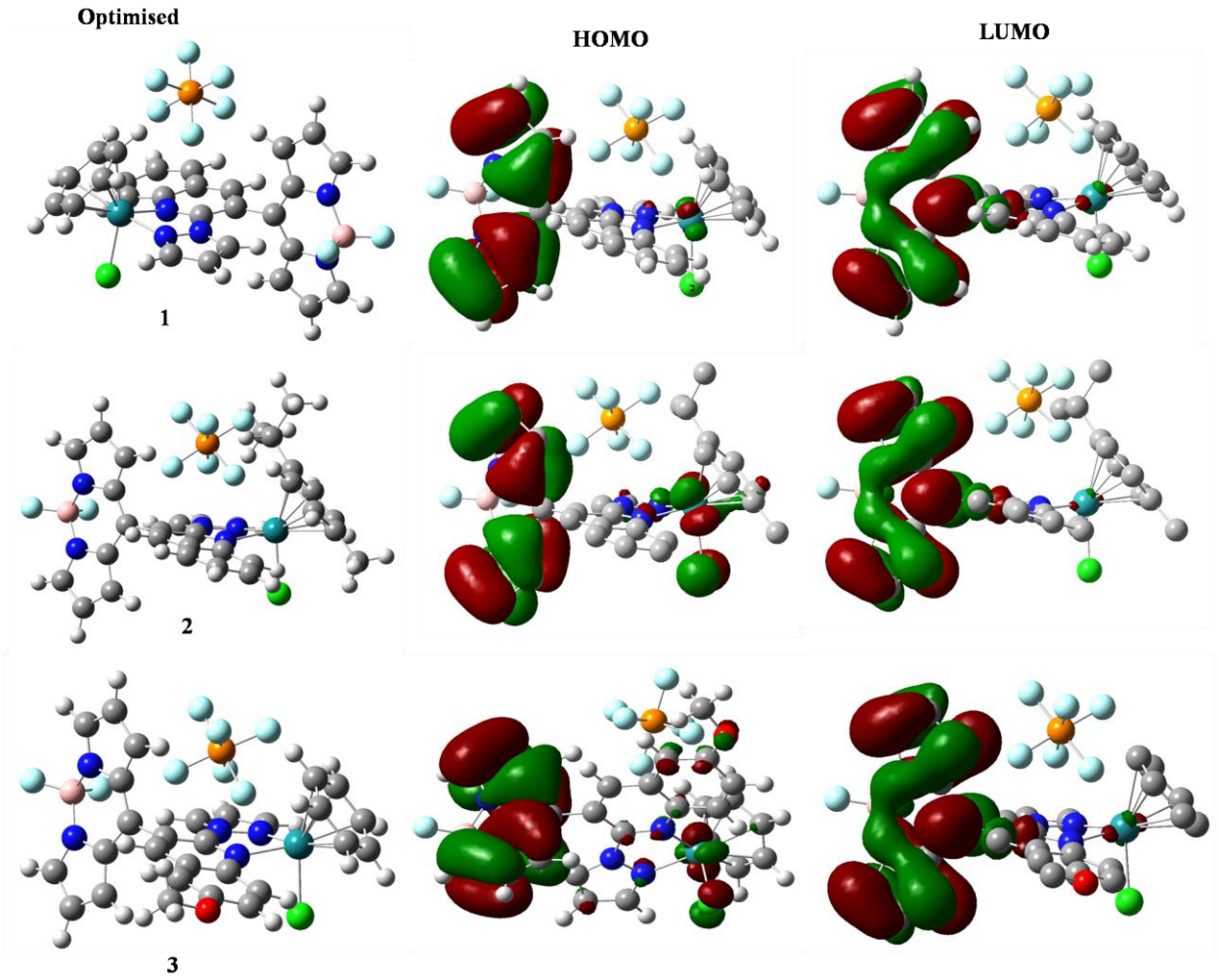

Fig. S18 DFT optimised structures and Frontier MOs contour plots for complexes **1–3.**

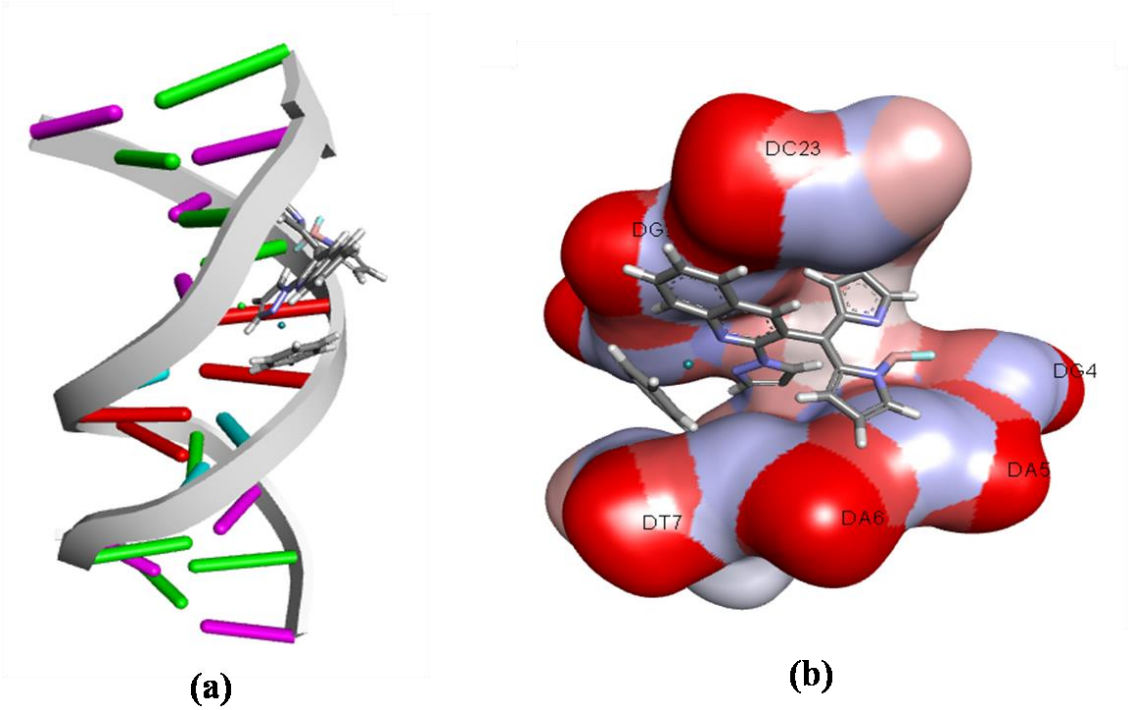

Fig. S19 Molecular docked model for complex **1** with DNA (PDB ID: 1BNA). Open (left) and closed (right) view of the docked model.

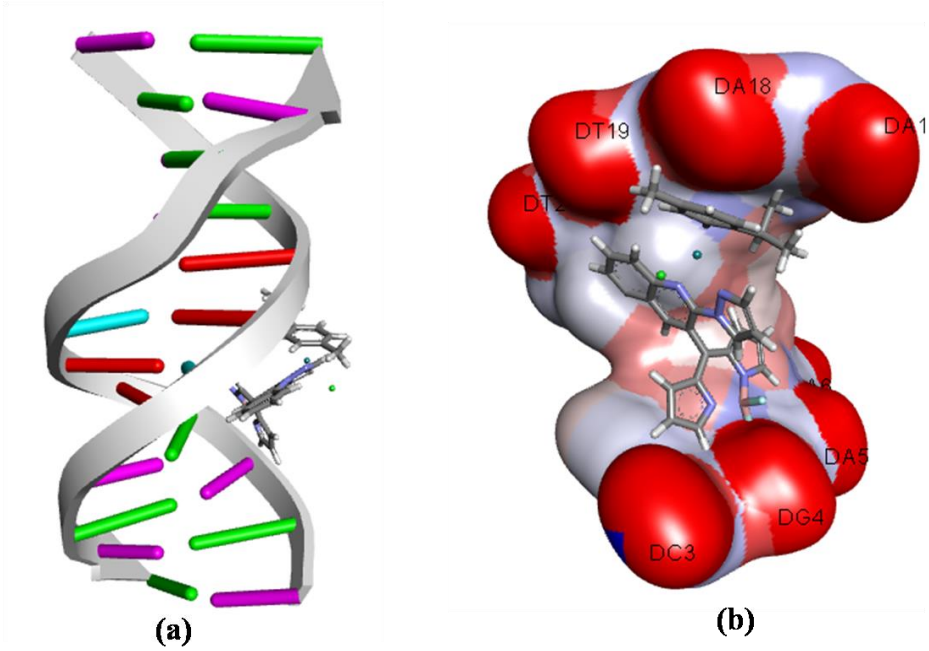

Fig. S20 Molecular docked model for complex **2** with DNA (PDB ID: 1BNA). Open (left) and closed (right) view of the docked model.

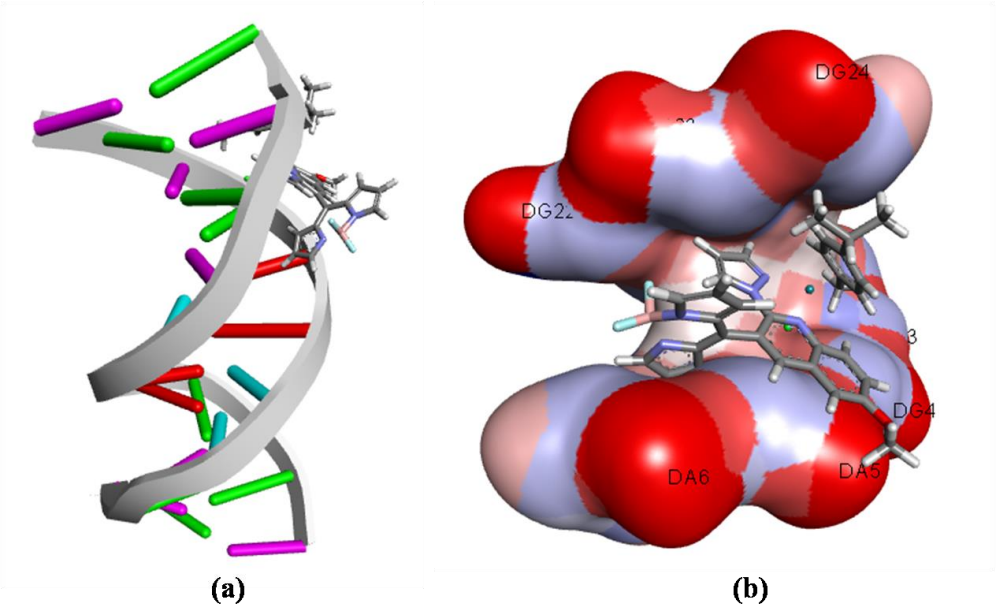

Fig. S21 Molecularky docked model for complex **3** with DNA (PDB ID: 1BNA). Open (left) and closed (right) view of the docked model.

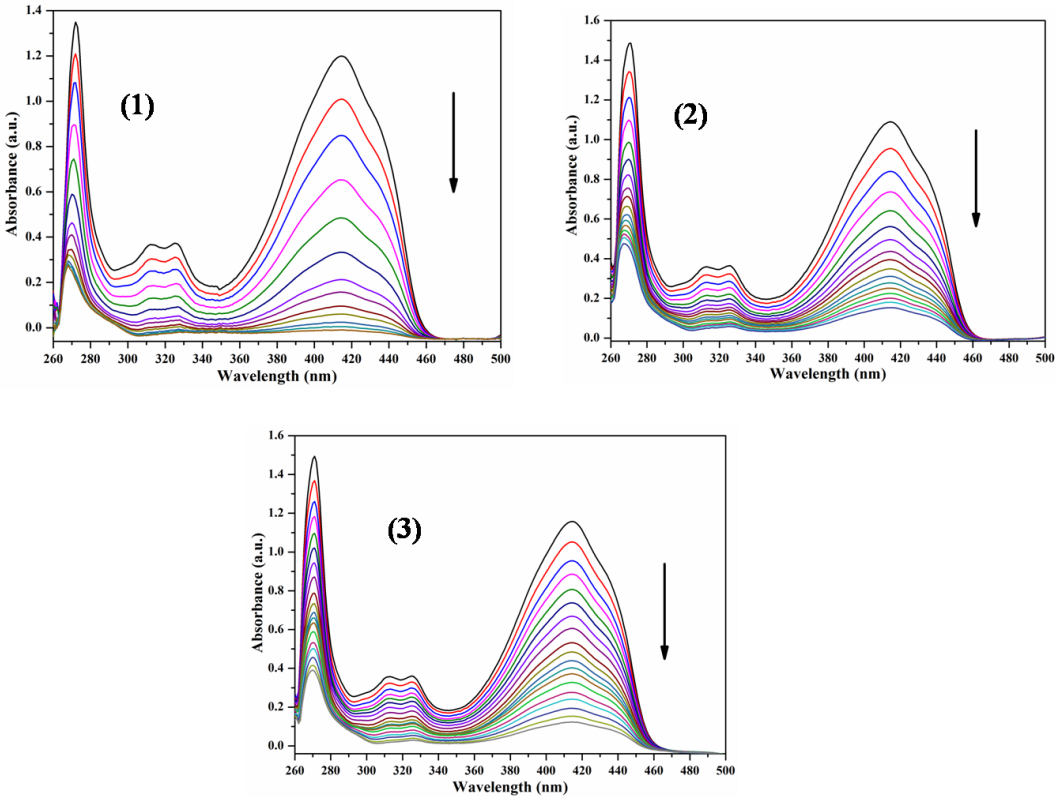

Fig. S22 Absorption spectral changes for DPBF and complex **1–3** (5 μM) upon exposure to visible light (400−700 nm, 10 J cm^{-2}) after 5 s interval.

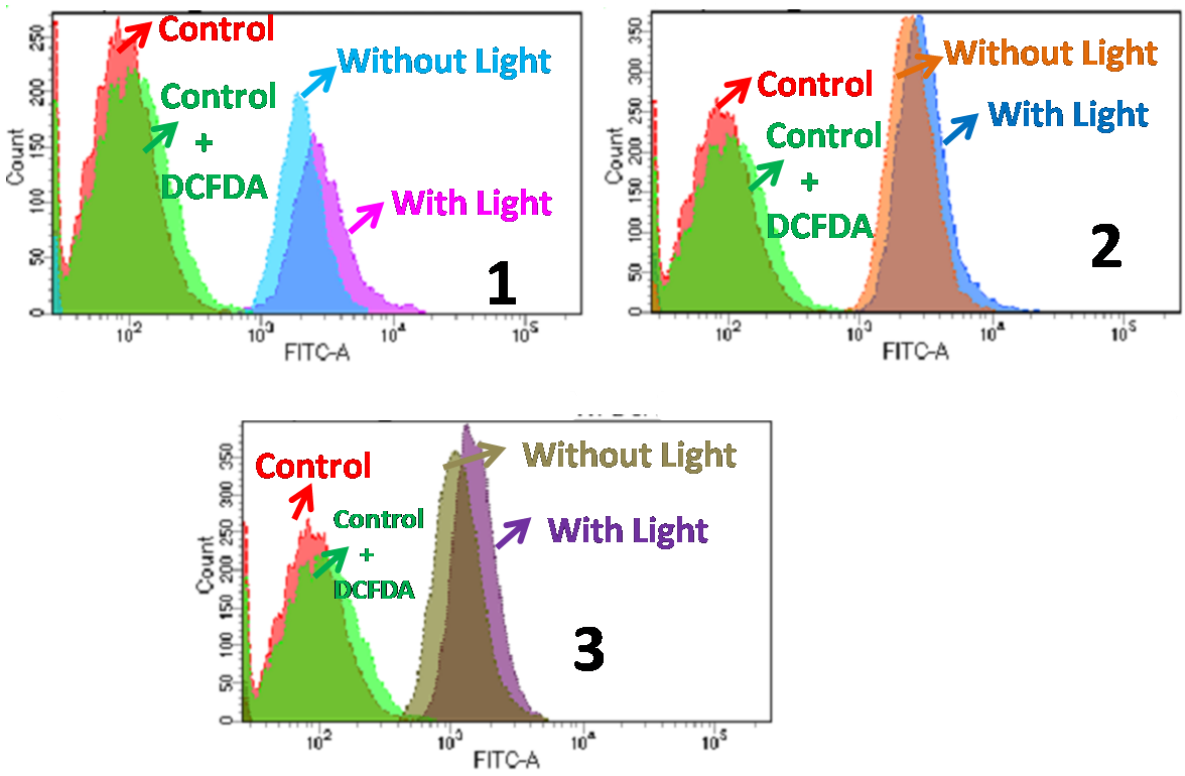

Fig. S23 Flow cytometer analysis of DCFDA in the presence of complex **1–3** upon exposure of visible light on HeLa cells.

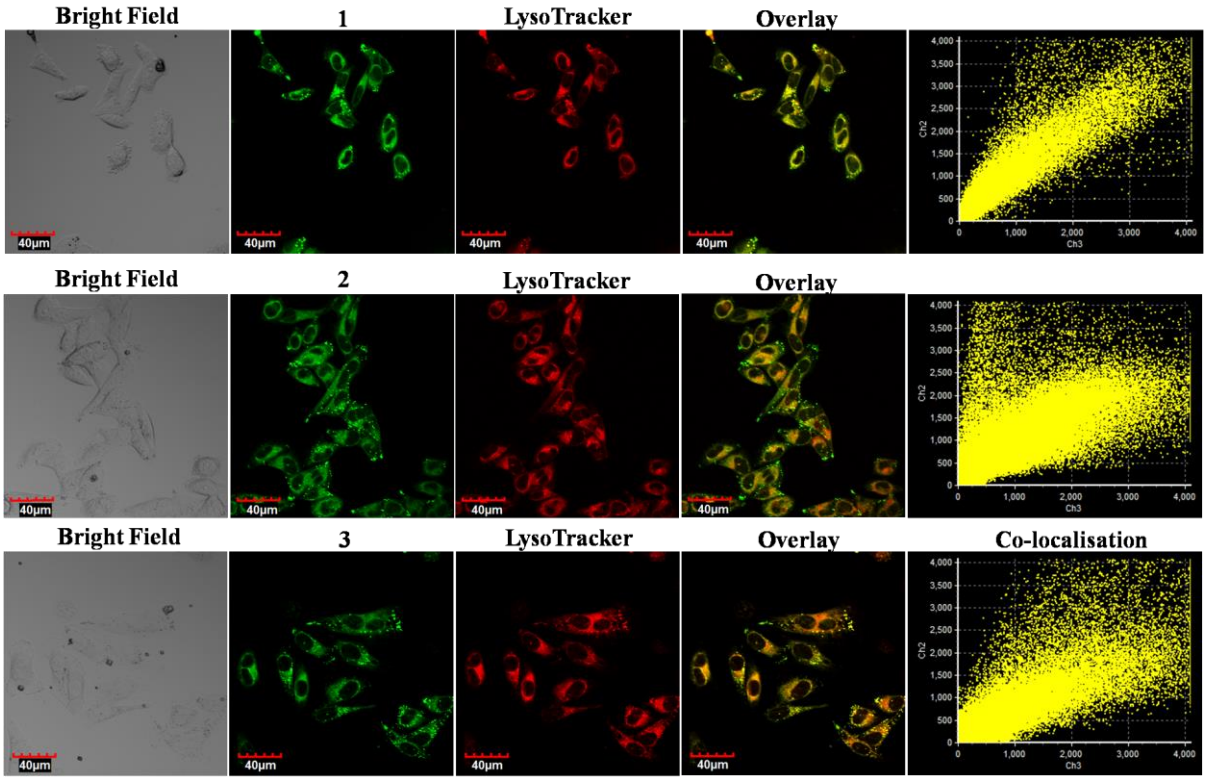

Fig. S24 Fluorescence microscopic images of HeLa cells in the presence of complexes **1–3** using LysoTracker Red (Scale bar–40µm).

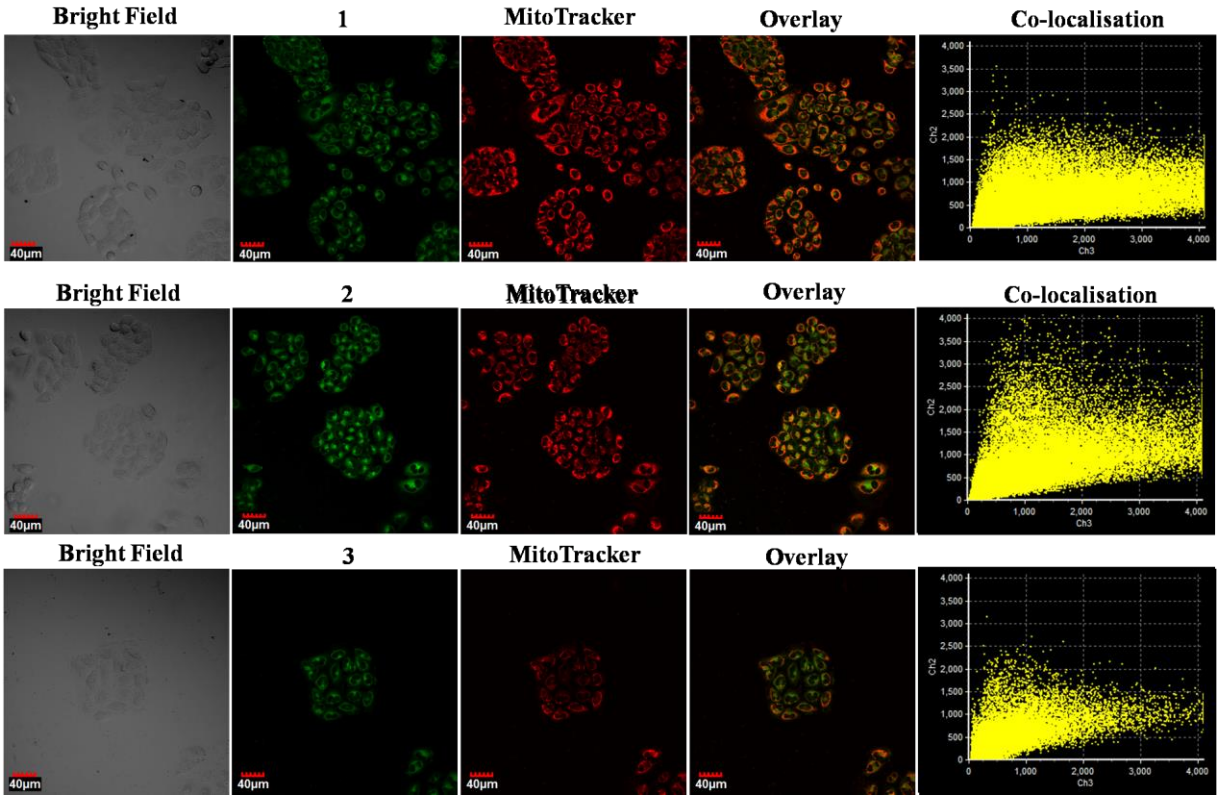

Fig. S25 Fluorescence microscopic images of HeLa cells in the presence of complexes **1–3** using MitoTracker Red (Scale bar–40µm).

Table S1. Selected bond lengths (Å) and angles (˚) for **L1, 1** and **4.**

Bond length (Å)	**L1**	**Bond length (Å)**	**1**	**Bond length (Å)**	**4**
B1–N1	1.533	Ru1–N3	2.160	Ru1–N3	2.130
B1 –N2	1.549	Ru1–N5	2.040	Ru1–N5	2.064
B1 –F1	1.377	Ru1–Cl1	2.398	Ru1–Cl1	2.387
B1 –F2	1.377	Ru1–C*g*	1.685	Ru1–C*g*	2.199
C5 –C10	1.483	Ru1–C*av*	2.189	Ru1–C*av*	1.683
Bond Angle (˚)		**Bond Angle (˚)**		**Bond Angle (˚)**	
N1– B1–N2	105.87°	N3– Ru1–N5	75.40°	N3– Ru1–N5	74.77°
F1– B1–F2	109.76°	N3– Ru1–Cl1	85.26°	N3– Ru1–Cl1	86.92°
N1– B1–F1	110.57°	N5–Ru1–Cl1	84.31°	N5–Ru1–Cl1	87.55°
N2– B1–F2	110.17°	C*g*– Ru1–Cl1	130.51°	C*g*–Ru1–Cl1	128.60°
N1– B1–F2	110.46°	C*g*– Ru1–N3	134.08°	C*g*–Ru1–N3	131.65°
N5– B1–F1	109.96°	C*g*– Ru1–N5	127.70°	C*g*–Ru1–N5	129.42°

Table S2: Changes in UV-Vis of **1–4** increasing concentrations of CT-DNA (0–20 μM) at room temperature.

Complex	λ_{abs} (nm)	Changes in molar extinction coefficient ε ($M^{-1}cm^{-1}$) X 10^4	% Hypochroism
1	512 336	4.51–3.80 2.02–1.76	15.7% 12.8%
2	511 339	6.00–5.00 2.57–2.20	16.6% 14.4%
3	512 346	6.05–5.07 2.76–2.39	16.1% 13.40%
4	511 349	5.54–4.52 2.28–1.95	18.4% 14.5%

Table S3. Log *P* Values for the complexes **1**–**4.**

Log P		
Complex	**Mean**	**SD**
1	0.90	0.02
2	0.84	0.03
3	0.77	0.02
4	0.69	0.02

Results are the means of three independent experiments and are expressed as means ± SDs.

Table S4. Fluorescence lifetime and electrochemical data of ligands **L1–L2** and complexes **1**–**4** in acetonitrile.

Compound	**λ_{em} (nm)**	**Quantum yield (%)**	**$<\tau_{avg}>$ (ns)**	**E_{pc}, (V)**
L1	520	18	0.75	–0.85
L2	521	13	0.95	–0.90
1	528	3.9	0.55	–0.75
2	530	6.4	0.50	–0.80
3	529	3.9	0.65	–0.82
4	530	4.1	0.35	–0.86

Fluorescence quantum yield in acetonitrile solution estimated using Rhodamine 6G as standard (Φ_F = 95% in water).

Table S5: Kinetic data for the hydrolysis of complex **2** and **4** monitored by UV-Vis at 298 K at dark(a; up to 12 h) and light (b; up to 2 h; 400−700 nm, 10 J cm^{-2})

Compound	**$k(min^{-1})^a$**	**$t_{1/2}(min)^a$**	**$k(min^{-1})^b$**	**$t_{1/2}(min)^b$**
2	0.00045	1540	0.002	346.5
4	0.00060	1155	0.003	231